Radiative Forcing and Climate Sensitivity of Carbon Dioxide (CO₂) Fine-tuned with CERES Data

Antero Ollila [a*]

[a] *Department of Civil and Environmental Engineering (Emer.), School of Engineering, Aalto University, Espoo, Otakaari 1, Box 11000, 00076 AALTO, Finland.*

Author's contribution

The sole author designed, analyzed, interpreted and prepared the manuscript.

Original Research Article	***Received: 26/09/2023*** ***Accepted: 30/11/2023*** ***Published: 05/12/2023***

ABSTRACT

An updated effective radiative forcing (ERF) value for constructing a simplified logarithmic forcing equation, and a transient climate response (TCR) value, are presented for CO_2, CH_4, and N_2O. The results are based on line-by-line (LBL) calculations utilizing the HITRAN database and the CERES radiation flux data for fine-tuning. The ERF value derived when doubling the CO_2 concentration from 280 ppm ($2xCO_2$) is 2.65 Wm^{-2} which is in line with the instantaneous radiative forcing (IRF) values of climate models referred to by the IPCC. The difference between the ERF values comes from the stratospheric cooling effect. It is a question about an essential paradigm change of the IPCC approach. In the former $2xCO_2$ value of 3.7 Wm^{-2}, its portion was about 5 %, and in the present value, it is about 30 %. According to this study, the same effect is 10 %. The updated TCR value is 0.7 ±0.15 °C.

_____

Corresponding author: E-mail: aveollila@yahoo.com;

1. INTRODUCTION

1.1 Radiative Forcing of Carbon Dioxide

The ERF of CO_2 is the largest driver in ongoing global warming, according to the prevailing paradigm in climate science. The specification of ERF has been changed in almost every IPCC report and the differences between the AR5 and AR6 will be analyzed in detail. The common measure for the CO_2 warming effect is climate sensitivity, which has been defined as equilibrium climate sensitivity (ECS) and as transient climate sensitivity (TCS), which is practically the same as the present-day term transient climate response (TCR). The IPCC [1] concluded in the AR5 that *"TCR is a more informative indicator of the future climate than ECS"*, and TCR determines the warming expected over a 50- to 100-year time scale. Therefore, in this study, only the TCR dependence on the ERF values of CO_2 has been evaluated. The term $2xCO_2$ has been used to denote the ERF value of a doubled CO_2 concentration from 280 ppm to 560 ppm. This chapter is background information and analysis of the present IPCC's understanding of the radiative strengths of greenhouse (GH) gases, and the magnitude of the TCR. The analyses of this chapter detail the problems and incoherences in the referred research studies as well as in the AR6 [2].

1.1.1 Radiative forcing specification of the AR5

The RF value calculated at the tropopause was called instantaneous radiative forcing (IRF) in the AR5, and at the top of the atmosphere (TOA), the IPCC [1] used the term effective radiative forcing (ERF) to represent the change in net TOA downward radiative flux after allowing for atmospheric temperatures, water vapor and clouds to adjust, but with global mean surface temperature or a portion of surface conditions unchanged.

The IPCC applied in the three earlier assessment reports TAR [3], AR4[4], and AR5[1] an Equation (1) from Myhre et al. [5] which gives a $2xCO_2$ of 3.71 Wm^{-2}:

$$ERF = k * \ln(C/280) \qquad (1)$$

where k is 5.35 and C is the concentration of CO_2 in ppm. According to the data of [5], the cloudy-sky RF broadband model value of 1.322 Wm^{-2} is about 27% lower than that of the clear-sky value of 1.800 Wm^{-2}. Myhre et al. [5] calculated that in the year 1997 CO_2 (concentration 363.9 ppm) and the shortwave (SW) absorption in the stratosphere caused RF of +0.11 Wm^{-2}. This SW absorption increased the stratospheric temperature and hence the RF of LW absorption was reduced to -0.05 Wm^{-2} resulting in the net stratospheric cooling effect of +0.06 Wm^{-2}. Since the total RF follows logarithmic dependence, the same can be applied to the RF effect by SW radiation, and the ERF by $2xCO_2$ would be 0.16 Wm^{-2}. Based on these estimates, the IRF would be 3.71 Wm^{-2} - 0.16 Wm^{-2} = 3.55 Wm^{-2}. Hence, stratospheric cooling increases the IRF value by about 4.5%, according to Myhre et al. [5], but this is a rough estimate since more accurate values are not available. It should be noticed that this LW cooling originates from SW warming in the stratosphere according to Myhre et al. [5].

1.1.2 Stratospheric cooling and warming effects

The stratospheric cooling effect was introduced in 1967 by Manabe and Wetherald [6]. In the historical evolution review study of the radiation forcing concept, Ramaswamy et al. [7] concluded that a CO_2 increase will cause increased emittance of the stratosphere, which leads to cooling. Goessling and Bathiany [8] formulated the same thing "The excess of emission compared to absorption leads to a cooling."

The increased CO_2 concentration reduces LW radiation from the troposphere into the stratosphere and further LW radiation from the stratosphere will reduce; this is the basic phenomenon of the radiative forcing concept. Without accurate LBL calculations, it is not self-evident that LW radiation change from the stratosphere is greater than the same from the troposphere in the case of $2xCO_2$.

Stratospheric temperature-adjusted radiative forcing (SARF) is defined in AR6 as the change in the net radiative flux at TOA following a perturbation including the response to stratospheric temperature adjustments [2, p.941]. In this paper, the terms SARF and stratospheric cooling have been used interchangeably.

Ramaswamy et al. [7] have noticed that the SW absorption by CO_2 reduces the solar absorption at the surface and causes a weak change at the TOA. This statement does not express how much of this SW absorption happens in the

stratosphere and what is its warming effect in the stratosphere. It looks like Myhre et al. [5] are the only ones who have considered SW warming in the stratosphere and have shown at least one numerical value. The literature survey reveals no research study indicating real numerical values about SW warming and LW cooling effect in the stratosphere carried out by LBL calculations.

The results of Ohmura [9] show that the total LW absorption develops very rapidly: 10 m 34 %, 100 m 67 %, 1 km 89 %, and 2 km 95 %. The results of Ollila [10] are similar for 1 km and 2 km and the absorption at the tropopause is 98 %. The quantitative research results of LW absorption by CO_2 according to altitude are almost nonexistent. Ramaswamy et al. [7] state that "*for carbon dioxide, the main 15-μm band is saturated over quite short distances*." One can assume that 'short distances' would mean probably a hundred meters rather than kilometers. Ollila's result [10] is that the CO_2 absorption is saturated below 1 km altitude. The research studies of Myhre et al. [5], Etminan et al. [11], Meinshausen et al. [12], and Smith et al. [13] do not refer to this issue at all. One of the key issues thinking stratospheric cooling is in which way the saturated CO_2 absorption below 1 km altitude can affect the total absorption happening in the stratosphere, and this will be analyzed in detail.

It is generally accepted that in the stratosphere reduced LW absorption causes a cooling effect and increased SW absorption causes a warming effect. If the sum of these effects is a cooling effect, it is essential to assess what is the change in the radiative flux at TOA. Huang and Ramaswamy [14] have calculated the absorptivity effect and the Planck effect (emission rate) in the troposphere. The absorption in the gas phase increases in lower temperatures but at the same time emissivity decreases and the result is largely one of cancellation. The same radiation laws are applicable also in the stratosphere.

1.1.3 Radiative forcing specification of the AR6

The IPCC has changed the terminology and the specifications of RF terms in the AR6 [2]. The IRF is defined as the change in the net TOA radiative flux following a perturbation, excluding any adjustments.

The ERF is the final RF at the TOA for a particular forcing agent, and it is the sum of the IRF and the adjustments. The ERF can be constructed bottom-up by calculating the IRF and adding in adjustments one-by-one or together. These adjustments can be referred to as rapid adjustments originating from the troposphere and the land surface, and they occur during periods from weeks to months. Slower adjustments are called climate feedback, and include ice/albedo, lapse rate, water vapor, and cloud feedback; they are not included in the ERF calculations [13]. According to the AR5 [1], water vapor increase due to anthropogenic emissions forcing occurs in all climate models, and it is not recognized as a form of radiative forcing but as climate feedback.

This new paradigm for ERF calculations has been introduced and applied in many global climate models (GCMs). Chung and Soden [15] introduced the so-called kernel method, which includes a few adjustments with a linear effect on the ERF:

$$ERF = IRF + A_T + A_S + A_{TS} + A_W + A_A + A_C + E \qquad (2)$$

where A_X is a rapid adjustment due to tropospheric temperature (T), stratospheric temperature (S), surface temperature (TS), water vapor (W), surface albedo (A), and clouds (C), and E is a residual that accounts for nonlinearities. One should notice that $SARF = IRF + A_S$. For some reason, the term "GH effect" cannot be found in the paper of Chung and Soden [15].

1.1.4 Calculation of ERF values in the AR6

The ERF calculations of AR6 [2, Ch 7.3] are based on the material of [13] who applied the kernel method, utilizing 11 different GCMs for calculating IRF and ERF values. The numerical values cannot be found in their paper except for the cloud adjustment of 0.45 Wm^{-2}. The author of this study estimated the adjustments from the graphical Fig. in [13], and these terms are in the same order as in Equation (2) in the calculation of the ERF:

$$ERF = 2.60 - 0.58 - 0.22 + 0.22 + 0.11 + 0.44 + 1.12 = 2.60 + 1.1 = 3.7 \qquad (3)$$

The dominant adjustment turns out to be the stratospheric temperature adjustment A_S (1.12 Wm^{-2}) since the sum of other adjustments in Eq. (3) is near zero (-0.03 Wm^{-2}). The most striking feature of this calculation method is that the IRF is only 2.6 Wm^{-2}, based on the 11 climate model calculations at the TOA.

In its latest report, AR6 [2], the IPCC used the calculations of [13], but the ERF value is different. The final reported ERF value can be found in Table 2 and Table 4 of the AR6 [2]. In Table 2 the average ERF value of 10 GCMs is 3.73 Wm^{-2}, and it is remarkably close to 3.7 Wm^{-2} of eq. (3) of [5].

The final of AR6 is 3.93 Wm^{-2}. The explanation is according to AR6 [2, p. 945] "*The 2xCO2 ERF estimate is 0.2 W m^{-2} larger than using the AR5 formula [5, pp. 659-740] due to the combined effects of tropospheric adjustments which were assumed to be zero in AR5*".

Table 4 of [2] is another presentation of the ERF value calculation and it is done by modifying Equation (2) using SARF instead of IRF and adding the tropospheric adjustments resulting in the average values of 10 GCM simulations: ERF = SARF + total tropospheric adjustments. Total tropospheric adjustment = tropospheric adjustment + water vapor adjustments + cloud adjustment + surface albedo & land-cover adjustment.

$$ERF = 3.75 - 0.60 + 0.22 + 0.45 + 0.11 = 3.75 + 0.23 - 3.75 + 0.18 = 3.93 \pm 0.47 \ Wm^{-2} \quad (4)$$

The total tropospheric adjustment of 0.18 Wm^{-2} differs slightly from the sum of its elements of 0.23 Wm^{-2} since the adjustments due not sum linearly according to Table 4 [2] explanation. The "official" tropospheric adjustment value of 0.2 Wm^{-2} is between these two values.

In [2] the SARF value of 3.75 Wm^{-2} differs slightly from the Table 2 value of 3.73 Wm^{-2} without any explanation. If the IPCC could have used the value 3.73 Wm^{-2}, then the tropospheric adjustment of 0.18 Wm^{-2} would have been 0.2 Wm^{-2}, which would match the general explanation on page 941 of AR6 [2]. These small numerical discrepancies make it rather difficult to follow the calculations of the AR6.

Four observations can be made.

Firstly, the IPCC [2] did not use Equation (2), applying the IRF value as a starting point, but formulated a new presentation not found in any scientific paper, since they replaced IRF with SARF. This approach means that the IPCC has formulated a new paradigm, and the ERF of 3.93 Wm^{-2} is about 0.2 Wm^{-2} greater than the SARF values in the referenced studies: 3.7 Wm^{-2} in Smith et al. [13] and 3.75 Wm^{-2} in

Meinshausen et al. [12]. The difference originates from the omittance of the surface temperature adjustment A_{TS} of -0.20 Wm^{-2}. The IPCC [2] has eliminated A_{TS} since the ERF is determined by the change in the net downward radiative flux at the TOA after the system has adjusted to the perturbation but excludes the radiative response to changes in surface temperature. The scientific basis is justified but the IPCC has broken its own rules that it uses only reviewed scientific papers without carrying out its own scientific research work. The ERF value of 3.93 Wm^{-2} cannot be found in any referred papers of the AR6 even though the surface temperature adjustment A_{TS} of about -0.20 Wm^{-2} can be found in the calculations of Smith et al. [13].

Secondly, the only numerical adjustment value, which can be found in the paper of Smith et al. [13] is $A_C = 0.45 \ Wm^{-2}$. It is unclear from which source the IPCC has taken the other numerical adjustment values in Table 2 [2] but they are close to the graphical presentations, which have been used in Equation (3). Probably these values are from personal data requests.

Thirdly, the IPCC [2] did not use the new paradigm of Chung and Soden [15], in which it was found that about 30% of the radiative forcing of 2xCO₂ happens in the stratosphere. In Table 3 [2] the portion of stratospheric cooling is also reported to be 30 % according to Smith et al. [13]. It looks like the IPCC does not want to pay attention to the real numerical magnitude of IRF (2.6 Wm^{-2}) and the stratospheric adjustment of 1.12 Wm^{-2} (~ 0.3*3.73 Wm^{-2}). This means that readers of the AR6 may have no clear idea about the magnitude of the stratospheric adjustment in the final ERF value. The IRF of 2.6 Wm^{-2} at the TOA looks illogical if compared to the IRF of 3.55 Wm^{-2} at the tropopause in the AR5. There is no information or analyses in AR6 [2], what are the IRF calculation methods applied in the GCMs. Smith et al. [13] report that IRF is not known precisely from many models, which were applied in their ERF simulations. This sounds odd since the IRF's portion is still about 70 % of the ERF.

Fourthly, The IPCC [2] carried out its GCM calculations by utilizing the data from the 10 GCM simulations of Smith et al. [13], and the results are summarized in Table 2 [12]. One GCM model (namely, ECHAM6-HAM2) has been left out, and some other changes have been made. The ERF values in Table 2 of the AR6 [2]

calculations vary from 3.45 Wm^{-2} to 4.27 Wm^{-2} creating the multi-model mean and 5 % – 95 % confidence range of 3.93±0.48 Wm^{-2}. This result is almost the same as 3.93±0.47 Wm^{-2}, which is the official ERF of the AR6 [2], but it is different from the ERF of 3.7 Wm^{-2} obtained via the 11 GCM simulation runs of Smith et al. [13]. The difference that has been explained above is the elimination of the tropospheric adjustments. A question can be raised if the result would be different by selecting different GCMs.

The IPCC does not analyze the significant differences between the AR5 and AR6: IRF 3.55 Wm^{-2} versus 2.6 Wm^{-2}, and stratospheric cooling values 0.16 Wm^{-2} versus 1.12 Wm^{-2}. If the ERF definitions and calculations of the IPCC look unclear and complicated, the presentations of the IPCC should be blamed in the first place.

1.2 Analysis of Other ERF Calculations

Etminan et al. [11] updated the original calculations of Myhre et al. [5] using the latest HITRAN [16] database version 2016, LBL calculations, and the latest atmospheric data. The LBL method uses the Oslo LBL code, which was also used by Myhre et al. [5], but has now been updated to include clouds, SW absorption, and stratospheric temperature adjustment [17]. The calculated SARF value can be estimated to be 3.75 Wm^{-2}, the same as in Meinshausen et al. [12], who used the same data, although their fitting equation gives slightly different values for very high CO_2 concentrations above 2000 ppm.

Ollila [18] calculated the ERF value at the TOA utilizing the LBL code of the Spectral Calculator [19] without a stratospheric cooling effect. The simplified equation has the same logarithmic form as in Eq. (1), but the parameter k = 3.12, which leads to the value of 2.16 Wm^{-2} of $2xCO_2$. This value is a combination of the clear-sky value of 2.69 Wm^{-2} and the cloudy-sky value of 1.88 Wm^{-2}, without any adjustments. Hence, the cloudy-sky value is 30% lower than the clear-sky value, which is close to the cloudy-sky reduction of 27% given by Myhre et al. [5].

The ERF values of [5], [11], and [12] are close to each other: 3.71, 3.75, and 3.75 Wm^{-2}, respectively. There is one difference in the calculation methods. The ERF of [5] is based on spectral calculations at the tropopause with stratospheric adjustments originating from SW warming. The ERF of [11], and [12] are based on

spectral calculations by the OSLO LBL model at the TOA including the effects of clouds and stratospheric cooling but the surface temperature has not been changed. It means that these RF results correspond to the ERF specification.

Wijngaarden and Happer [20] published GHG forcing and warming effect calculations. In their paper, they provide a detailed description of their own LBL calculations, which are not based on any publicly available codes or applications. They used the latest 2016 database of HITRAN [16], and the results are based on calculations with no water continuum model, and without any stratospheric cooling effects. Their RF value for $2xCO_2$ (from 400 ppm to 800 ppm) is 3.0 Wm^{-2} at the altitude of 86 km, and the same value at 11 km is 5.5 Wm^{-2}. A possible conclusion is that in the stratosphere the RF effect decreases by 2.5 Wm^{-2}, but according to Smith et al. [13], it should increase by 1.12 Wm^{-2}.

Harde [21] also applied his own LBL calculations and his two-layer atmospheric model. His RF value for $2xCO_2$ is 2.4 Wm^{-2}. Miskolczi and Mlynczak [22] carried out extensive LBL calculations with different atmospheric compositions, and their $2xCO_2$ value is 2.53 Wm^{-2}.

1.3 Climate Sensitivity Parameter, Climate Feedback Parameter, and TCR

The surface temperature values can be calculated using a simple equation (5), as defined by the IPCC [1, p.664] and it was formulated for a case from a climate equilibrium state to another equilibrium state. It may sound like it is applicable only for the equilibrium climate sensitivity (ECS) calculations. The later examples show that it has been usually applied for TRC calculations and more generally for temperature change calculations during this century.

$$dTs = \lambda * RF \qquad (5)$$

where dTs is the global mean surface temperature change, and λ is the "climate sensitivity parameter". The transient climate response (TCR) is defined as "*the change in the global mean surface temperature, averaged over 20 years, centred at the time of atmospheric carbon dioxide doubling, in a climate model simulation*" in which the atmospheric CO_2 concentration increases at 1% per

year. That estimate is generated by using shorter-term simulations.

The earlier λ values of the IPCC were taken from the study of Ramanathan et al. [23], based on eight research papers giving an average value of 0.5 K/(Wm^{-2}), varying from 0.47 K/(Wm^{-2}) to 0.53 K/(Wm^{-2}). Table 5 of the AR4 [4] is a summary of the ECS and TRC values of 30 GCMs and it reveals that the model mean average value λ for ECS is 1.0 K/(Wm^{-2}), and the arithmetic average is 3.2 °C /

3.7 Wm^{-2} = 0.86 K/(Wm^{-2}). It means that according to the IPCC, Eq. (5) is applicable for TRC- and ECS-type calculations. When Syuruko Manabe was awarded the Nobel Prize for Physics in 2021, one of Manabe's main credits was that Manabe and Wetherald [6] were the first to introduce positive water feedback. The conclusion was that water feedback doubles the original RF of CO_2, and the λ value was 0.53 K/(Wm^{-2}). This quality became one of the essential features of GCMs as early as the 1980s.
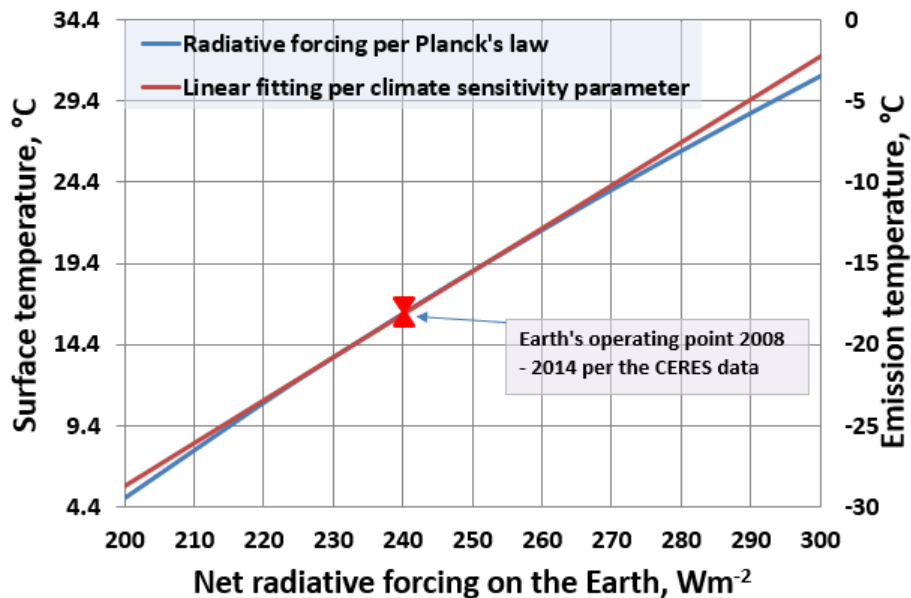

Fig. 1. Emission temperature dependency according to Stefan-Boltzmann law and according to linear dependency per Eq. (7)
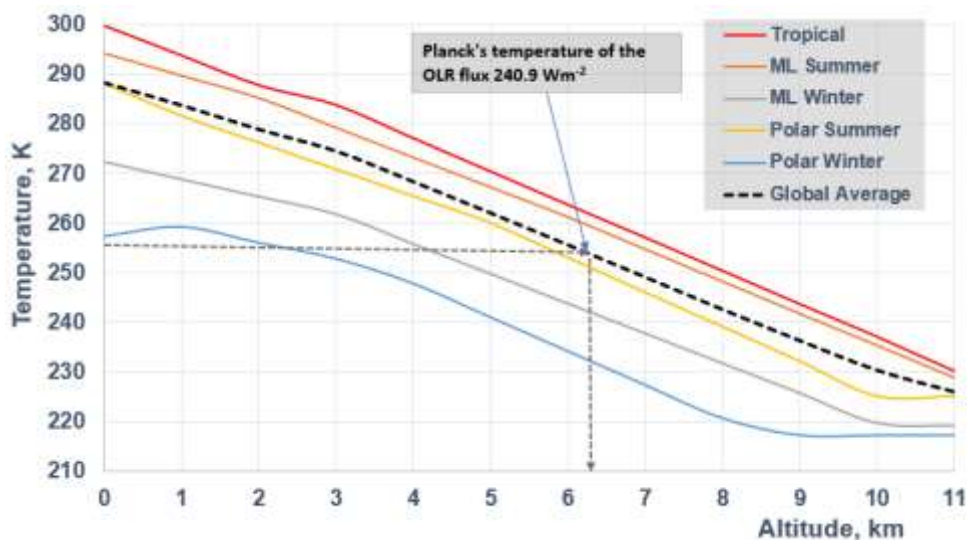

Fig. 2. Emission temperature according to Planck's law in the present climate

The λ value of 0.5 K/(Wm^{-2}) was also found in assessment reports 3 and 4 of the [3] and [4]. AR5 [5] did not specify the exact values but stated that water feedback amplifies any initial forcing by a typical factor between two and three. In Section 8.6.2.3 of AR4 [4], the IPCC reports that global warming would be around 1.2 °C if a constant water amount is applied in GCMs, which means a λ value of 0.32 °C/(Wm^{-2}). In AR6 [2] the IPCC changed its nomenclature and used the term "climate feedback parameter" α, which is the reciprocal of λ = 1/α. The feedback parameter α can be decomposed into different types of feedback, and the sum of feedback parameters is the direct relationship between the ERF and the global equilibrium surface temperature change.

Even though the IPCC [2] did not report a λ value for ERF in AR6, it can be calculated from the data in Fig. 6 and Fig. 7 of AR6, which are based on the GCM calculations. The ERF value of 2.70 Wm^{-2} (= total anthropogenic ERF 2.72 Wm^{-2} plus solar ERF -0.02 Wm^{-2}) results in a warming of 1.27 °C, meaning the λ value of 1.27 °C / 2.70 Wm^{-2} = 0.47 K/(Wm^{-2}), which is applicable in TCR calculations since the λ value of CO_2 is the same. The α value is 1/0.47 = 2.13 Wm^{-2}/K. This α value means that water feedback has been applied in the GCMs used for calculating warming values in Fig. 6.

Applying Eq. (5) gives the TCR value of 1.85 °C (= 0.47 °C/(Wm^{-2}) *3.93 Wm^{-2}), while the best estimate of AR6 [2] is 1.8 °C. For example, the dTs for the worst-case scenario SSP5-8.5 (shared socio-economic pathway) would be according to Equation (5), dTs = 0.47 K/(Wm^{-2}) * 8.5 Wm^{-2} = 4.0 °C. The average warming value according to the AR6 [2] is the same. These examples show that the average warming values calculated with the complicated GCMs can be calculated using Equation (5). Both the TCR and SSP scenario calculations, approved by the IPCC, assume that positive water feedback about duplicates the warming impacts of CO_2.

What is the relationship between the λ and the TRC, or are the TRC values calculated using λ close enough to TRC values as defined by the IPCC? Since the CO_2 growth rate is smaller than 1 % yr^{-1}, yearly temperature change dT calculations of present time and 2xCO_2 can be carried out by eq. (5). The dT effects from 1750 to 2019 in Figs 6 and 7 of AR6 have been carried out by GCMs including dynamical effects [2]. It turns out that the same dT values can be simply

calculated according to the equation dT = λ * ERF or ERF/α. This means that the results are the same when using Eq. (5) compared to the average results of several GCM simulations. The same applies to TCR calculations, as shown above: 1.85 °C using λ versus 1.8 °C using GCMs. This is possible since the time constant of dynamic delays in temperature response is shorter than one year. If this is not the case, the equation dT = λ * ERF would give different results.

Ollila [18] calculated the value of λ using three independent methods: via Earth's energy balance, the value is 0.268 K/(Wm^{-2}); via spectral calculations, the value is 0.259 K/(Wm^{-2}), and via the MODTRAN [24], the value is 0.319 K/(Wm^{-2}). These values mean that there is no positive water feedback mechanism, which is assumed in the case of a λ value of 0.47 K/(Wm^{-2}).

The theoretical justification of positive water feedback is based on the equation of Clausius–Clapeyron (C-C) This equation represents the pressure-temperature relationship in a saturated water vapor atmosphere. The real atmosphere is not saturated by water vapor, and therefore the theoretical basis is weak. Because the atmosphere's saturation is around 70% on average, one could think that anyway, the positive water feedback relationship would follow the C-C equation. This issue will be analyzed in detail in the Validation section based on the real temperature and humidity data. It turns out that the C-C relationship does not work in the real atmosphere.

1.4 Objectives of this study

The objectives of this study are to calculate the radiative forcing values of CO_2, CH_4, and N_2O by evaluating simplified RF equations. Special attention has been paid to ERF calculations and the stratospheric cooling issue. The TRC value has been updated based on the updated climate sensitivity parameter's value.

2. CLIMATE SENSITIVITY PARAMETER CALCULATIONS

In the study of Ollila [18], a mathematical expression for the climate sensitivity parameter λ was derived from the Earth's energy balance:

$$SC * (1- α) * (¶r^2) = εsT_e^4 * (4¶r^2) \qquad (6)$$

where SC is the solar constant, α is the albedo of the Earth, ε is emissivity, s is the Stefan–Boltzmann constant, and T_e is the average emission temperature of the outgoing longwave radiation (OLR). The emissivity of the Earth's surface can be approximated to be 1, and therefore it can be omitted

$$T_e = (SC(1-\alpha)/(4s))^{0.25} = 255.29 \text{ K} = -17.87 °C. \tag{7}$$

The term SC(1-α) is the net radiative forcing RF_{net} of the Earth, and Eq. (7) can be written $RF_{net} = sT_e^4$. When this Eq. is derived, it will be $d(RF_{net})/dT_e = 4sT_e^3 = 4RF_{net}/T_e$. By inverting this equation, λ will be

$$\lambda = dT_e/d(RF_{net}) = T_e/(4RF_{net}) = T_e/(SC(1-\alpha)) \tag{8}$$

Using the average CERES (2021) values for the period 2008–2014, λ = 255.29 K /(1360.04*(1-0.2916) Wm^{-2}) = 0.265 K/(Wm^{-2}). This value is close to the value of 0.27 K/(Wm^{-2}) calculated by Ollila [18].

Since λ gives the slope of a very nonlinear expression, there might be doubts if temperature change depends linearly on the ERF in the range of about +10 Wm^{-2} as needed in the SSP scenario calculations of the IPCC. In Fig. 1, the emission temperature is depicted as a function of the Stefan–Boltzmann law and according to Eq. (5), using the λ value of 0.265 Wm^{-2}. The deviation between these two curves is insignificant, and the numerical values show that in the ERF range from 230 Wm^{-2} to 250 Wm^{-2}, the error with these two equations is only 0.05 °C. This means that the linear Equation (2) using a constant λ value is sound when calculating the dT_e values of different ERF forcings.

The question is, what is the relationship between the emission temperature T_e and the surface temperature T_s? Normally, 33 °C is added to T_e when calculating the T_s. Using spectral calculations, the T_s value of 16.3 °C gives 240.7 Wm^{-2}, which is close enough to the observed CERES [25] value of 240.86 Wm^{-2} for the 2000s. This means that the temperature difference between the T_s and the T_e is 34.3 °C (the left axis in Fig. 1). What happens to this difference if small ERF changes occur due to GHG forcing effects? The temperature profiles of different climate zones according to [19] are depicted in Fig. 2.

The temperature profiles of climate zones behave in a near-linear way from the surface up to the tropopause, only the polar winter profile deviates more. This fact has been applied by estimating the lapse rate – the rate at which air temperature falls with increasing altitude – to be constant at 6.5 °C per kilometer. The lapse rate value has not been suggested to need modifying because of global warming. It can be estimated that, if the surface temperature increases even 4 °C, the temperature profiles would remain in the same mode, maintaining a linear relationship between the T_s and the T_e. The surface temperature differences between the climate zones range from -16 °C to 25.5 °C, and this situation shows that the profiles follow the same pattern over relatively large T_s differences. A conclusion is that a global temperature change dT_s will cause the same change in the average atmospheric temperature profile meaning that $dT_e = dT_s − 34.3$.

3. CLEAR, CLOUDY, AND ALL-SKY SIMULATIONS

3.1 Spectral Calculator Application

The author has used the spectral calculations tool application Spectral Calculator developed by Gats [19] in LBL calculations to simulate temperature and CO_2 concentration changes. This tool applies the latest HITRAN version [16], which is the high-resolution transmission molecular absorption database of the Harvard–Smithsonian Center for Astrophysics [16], and it now includes the water continuum model 2.52 MT_CKD of Mlawer et al. [26]. The author has modified the polar summer profiles of the Spectral Calculator [19] for temperature, pressure, and GHG concentrations to correspond to the average global atmosphere (AGA) profiles. Ollila [10] calculated the global total absorption value using these five different climate zones to be 307.53 Wm^{-2} in the troposphere. The same value when applying the adjusted polar summer profiles is 305.98 Wm^{-2}, which is only 0.5% smaller. It can be estimated that this small difference does not affect ERF calculations. Since the one profile calculation is so close to the five profile results, it is justifiable to use it in all LBL calculations in this study.

The Spectral Calculator LBL code together with the HITRAN database has been applied in numerous calculations without any problems or errors, according to Gats [19]. The number of

spectral lines originates from the HITRAN database, and spectra up to one million points can be calculated. The atmosphere is modelled as graduated concentric spherical shells. The number of shells depends on the path length and altitude range. For example, a path from the ground to 120 km (the top of our Spectral Calculator atmospheres) is split into 19 shells: 250 meters thick at the surface, growing to 10 km thick at high altitudes.

The author has applied the Spectral Calculator tool in his earlier studies [10] for calculating the contribution of CO_2 to the GH effect by applying the US Standard Atmosphere 1976 with 12% water reduction, and the result is 27% — almost the same as the 26% calculated by Kiehl and Trenberth [27]. Schmidt et al. [28] calculated that the CO_2 contribution to the GH effect is 14%, corresponding to 21.7 Wm^{-2} absorption, and these values, derived when applying the Spectral Calculator, are 12.7% and 20.1 Wm^{-2}, using GH effect magnitudes of 155 and 157.7 Wm^{-2}, respectively. Additionally, the total LW absorptions according to the altitude, derived with the Spectral Calculator, are the same as those reported by Ohmura [9]: 1 km, 90%; 2 km, 95%; 11 km, 98%.

3.2 Simulation of Cloudy-sky Conditions Applying CERES Data

In the earlier TCS calculations of Ollila [10,18], a problem arose, like in many other LBL codes, concerning the simulation of cloudy and all-sky conditions, because the Spectral Calculator LBL code is only applicable for clear-sky conditions. The cloudy-sky ERF and TCS values were calculated simply using 30% lower values with respect to clear-sky values. According to the data of Myhre et al. [5], the cloudy-sky ERF broadband model value of 1.322 Wm^{-2} is about 27% lower than the same clear-sky value of 1.800 Wm^{-2}. The newest ERF calculations have been derived using LBL codes, such as OSLO LBL [17], including cloud effects, and therefore the portion of clouds is not reported.

In this study, the radiation flux of the clouds and the CERES [25] data have been applied as reference material during the pause period from 2008 to 2014. This period has been selected since it contains no exceptional climate events, and it is long enough to filter out small deviations. The total precipitable water (TPW) amount [29] and [30] was 2.6 cm, the carbon

dioxide was 393 ppm, the methane concentration was 1.803 ppm, and the nitrogen oxide concentration was 324 ppb at the surface level on average.

The surface-emitted LW flux is 398 Wm^{-2}, according to the Earth's energy balance, when applying the CERES [25] radiation flux data during this reference period. This flux value corresponds to Planck's temperature of 16.3 °C. Huang et al. [31] analyzed five sea surface temperature (SST) datasets. During the pause from 2000 to 2014, the SST values varied from 18.1 °C to 18.5 °C. Since the oceans cover 70% of the Earth's area, the real surface temperature is higher than the 15 °C normally used as the global temperature estimate.

The average CERES-observed OLR values for this period are 240.038 Wm^{-2} for all-sky, and 267.940 Wm^{-2} for clear-sky, and the cloud fraction is 0.674. The cloudy-sky value is not readily available, but it can be calculated using the equation of Bellouin et al. [32].

$$OLR_{all-sky} = 0.674 * OLR_{cloudy} + 0.326 * OLR_{clear} \tag{9}$$

According to this equation, the OLR for a cloudy-sky is 226.54 Wm^{-2}. The clear-sky flux of 268 Wm^{-2} at the TOA is the sum of 186 Wm^{-2} radiated from the atmosphere, and 82 Wm^{-2} transmitted through the atmosphere. When the sky turns from a clear-sky to a cloudy-sky, the changes in radiation fluxes happen immediately. The transmittance flux of 82 Wm^{-2} disappears, and the atmosphere-radiated OLR of 226 Wm^{-2} becomes about 15.5% smaller than that of the clear-sky. This change is caused by the absorption of LW radiation by clouds, which plays an essential role in the GH effect.

The accurate ratio of OLR_{cloudy} to OLR_{clear} during the period 2008-2014 is 0.8455, which is marked as R_c in this study. The author has used R_c in calculating the cloudy-sky OLR values from the LBL-calculated OLR_{clear} values, which are required in ERF calculations of CO_2.

The absorption effect of CO_2 occurs below an altitude of 1 km since CO_2 is a strong absorber in its waveband zone. The global surface temperature under cloudy-sky conditions is about 0.1 °C higher than under all-sky conditions [33]. The explanation for this is that the increase in radiation from clouds is greater than the decrease in SW radiation to the surface during

relatively short periods of cloudy-sky conditions (about two days out of three are cloudy).

The average global cloud layer is at an altitude of 1.5 km to 4.1 km [34], and the LW absorption by CO_2 is completed below 1 km [10]. Thus, clear-sky LW radiation reduction for a specific CO_2 concentration is accurate enough for cloudy-sky reduction, but a reduction in OLR flux due to cloud absorption is required, which is proportional to OLR_{clear}, according to the coefficient R_c.

3.3 Stratospheric Cooling of CO_2 Using LBL Calculations

The effects of stratospheric cooling can be estimated reliably by applying the LBL calculation to the tropopause and the stratopause. In this study, the altitude applied in the calculations was 70 km, but the results are applicable for the stratosphere, since the H_2O, CO_2, and

O_3 concentrations do not vary from 50 km to 70 km, and the absorption saturation is almost complete; Therefore, the altitude range from 11 km to 70 km has been used in the stratospheric absorption calculations. The total absorption at the altitude of 50 km is only 0.17% smaller than the absorption at 70 km, which means that this altitude difference has an insignificant impact on stratospheric calculations.

Generally, the warming effects of SW absorption by CO_2 have not been included in ERF calculations. The only exception seems to be Myhre et al. [5], who have calculated that SW forcing in the stratosphere reduces the stratospheric cooling by about 46 % but in the troposphere the SW forcing effect is neglectable. The author has performed both the LW and SW absorption calculations in the stratosphere, and the results have been collected in Table 1.

Table 1. The LW and SW absorption effects (Wm^{-2}) in all-sky conditions in the stratosphere for CO_2 concentration changes

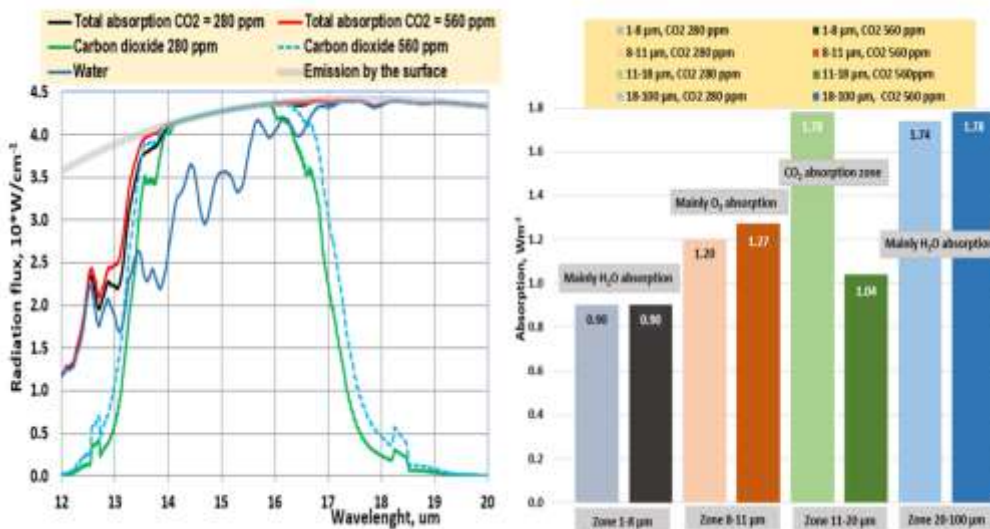| Item	280 ppm	393 ppm	560 ppm
OLR, 11 km	248.315	246.865	245.29
OLR, 70 km	242.704	241.537	240.304
LW absorption (11 km - 70 km)	5.611	5.328	4.986
LW absorption change	0	-0.283	-0.625
SW absorption change	0	0.168	0.360
Net cooling effect	0	-0.115	-0.265

Fig. 3. A. LW radiation absorption changes in the stratosphere in different wavelength zones per CO_2 concentrations of 280 ppm and 560 ppm. B. Total absorptions in the atmosphere (70 km) per CO_2 concentrations of 280 ppm and 560 ppm. The absorption curves of water and CO_2 concentrations of 280 ppm and 560 ppm correspond to the situation when there is only one gas at a time in the atmosphere

The figures in Table 1 show that the net effect of $2 \times CO_2$ in the stratosphere is -0.265 Wm^{-2} meaning a slight cooling since increased CO_2 concentrations decrease LW absorption in the stratosphere but the SW absorption increases. The stratospheric net cooling effects of Table 1 can be fitted by the logarithmic equation:

$$RF = 0.383 * \ln(C/280), \quad (10)$$

where RF is the net cooling effect of CO_2 in the stratosphere and C is the CO_2 concentration (ppm). The SW absorption reduces the LW cooling by about 58 % in the concentration of 560 ppm, which is rather close to 46 % of Myhre et al. [5] in the concentration of 363.9 ppm. The LBL calculations showed that the SW absorption of $2 \times CO_2$ in the troposphere is only 0.014 Wm^{-2} and it confirms the results of [5] that it can be omitted in ERF calculations.

Stratospheric cooling according to earlier studies [7] and [8] is caused by the excess of emission compared to absorption or it is caused by increased emittance of the stratosphere. The numerical values in Table 1 show that in the CO_2 concentration of 560 ppm, the OLR value of 240.304 Wm^{-2} (=emittance) is smaller than 242.704 Wm^{-2} of 280 ppm. Also, the net absorption in the stratosphere of the CO_2 concentration of 560 ppm is smaller than the absorption of the concentration of 280 ppm (4.986 Wm^{-2} versus 5.611 Wm^{-2}). Less absorption means less warming, i.e. stratospheric cooling.

As the numerical values in Table 1 indicate, there is a simpler explanation for stratospheric cooling by comparing the absorption values. The higher the CO_2 concentration, the smaller the LW absorption in the stratosphere. This fact is illustrated in Fig. 3.

As panel A of Fig. 3 indicates, the LW absorption growth by CO_2 concentration increase happens mainly through the widening of the CO_2 absorption peak in the wavelength zone from 12 µm to 14 µm, since the absorption from 14 µm wavelength onward is practically saturated due to the combined effects of water and carbon dioxide. Panel B of Fig. 3 shows that the absorption by CO_2 in the wavelength zone from 11 to 20 µm decreases in the stratosphere,

which is the main absorption zone of CO_2. As summarized before, the CO_2 is already saturated

below 1 km altitude, and therefore this decrease cannot be the direct effect of CO_2 absorption but is an indirect effect.

It should be noted the fact that water also absorbs LW radiation in this same zone. When the CO_2 absorption increases in the troposphere, less LW radiation enters the stratosphere mostly in the wavelength zone from 12 to 14 µm, and it means that less water absorption can happen in this wavelength zone. Ollila [35] has shown by LBL calculations that in the CO_2 concentration of 280 ppm, the total absorption in the stratosphere is divided between four GHGs: O_3 62.4 %, H_2O 36 %, and CH_4 & N_2O 2.6 %. In the CO_2 concentration of 560 ppm, the total LW absorption decreases by 0.625 Wm^{-2}, and the corresponding figures between four GHGs are O_3 69.0 %, H_2O 29.6 %, and CH_4 & N_2O 2.4 %.

The decrease of the total LW absorption in the stratosphere originates from the CO_2 absorption increase in the troposphere (below 1 km), which causes the reduction of water absorption in the stratosphere, and it also means the reduction of the total absorption in the stratosphere. A general radiation law states that less absorption means a cooling effect. The opposite happens in the troposphere where more absorption by CO_2 causes a warming effect. At the same time, it should be noticed that the total absorption from the surface to the stratopause will increase due to the strong tropospheric absorption by CO_2.

Bekki and Savarino [36] have shown that LW absorption does not explain the recent positive temperature gradient in the stratosphere. Most of the heat originates from the recombination of oxygen atoms with molecular oxygen due to the photolysis reaction caused by ultraviolet radiation below 242 nanometers. This very fast reaction releases 24 kcal of heat per mole of ozone formed. This result is in line with those of Philipona et al. [37], who analyzed stratospheric cooling based on radiosonde and satellite observations. They found that rising GHG concentrations and decreasing stratospheric ozone from the 1970s to the end of the century cooled the lower stratosphere. While ozone-depleting substance concentrations have decreased, ozone shortwave heating by increased O_3 concentration now contributes to warming. This change caused the cooling to stop around 2000, and since then, the lower

stratosphere has been slowly warming thanks to increased O_3 concentrations.

The analysis above shows that stratospheric cooling due to CO_2 concentration growth increases the final ERF value. This result is in line with the results of Myhre et al. [5] but it differs significantly from the stratospheric cooling of Smith et al. [13], and the IPCC [2]. The term "stratospheric temperature adjustment" has been widely used. This may create a mental image that the stratospheric temperature profile should be rectified to the original form to find the real temperature effect of 2xCO_2. It should be noted that there is no natural process, which could maintain or rectify temperature profiles. The driving force in the warming effect of GHGs changes is the reaction to the deviations in the Earth's energy budget, which must be in balance after dynamic delays. Temperature profile changes in the atmosphere depend on the radiation fluxes restoring the energy balance. This restoring effect originating from the 2x CO_2 will increase the surface temperature, which will increase the tropospheric temperature profile and decrease the stratospheric temperature profile as described above.

3.4 Spectral calculation results

The author has simulated the overall effects of GHGs and clouds using LBL calculations, and the results have been depicted in Fig. 4.

In Fig. 4, the transmission of surface-emitted radiation occurs in the region called the atmospheric window from 750 to 1250 cm^{-1}, because the water absorption is at the minimum in this wavenumber zone. The transmitted flux is 81.9 Wm^{-2}, and the radiated flux is 187.7 Wm^{-2}. In cloudy-sky conditions, the transmitted flux is zero. The black curve shows the OLR radiation that pertains to if the CO_2 concentration is zero. In some research like Wijngaarden and Happer [20], this absorption peak from 550 to 850 cm^{-1} has been claimed to be caused solely by CO_2, but the curves in Fig. 5 show that water has almost the same effect (about 40% of the total absorption) since they have overlapping absorption frequency bands.

The strong absorption peak in the atmospheric window zone from 1000 to 1100 cm^{-1} is due to ozone absorption mainly in the stratosphere. The 10% perturbations from the present climate's concentrations result in the following instantaneous relative strength values concerning carbon dioxide [10]: water 11.8. ozone 0.78. nitrogen oxide 0.14. and methane 0.11. In this respect, the global warming potential (GWP) values of [2] are rather misleading as regards the strength of greenhouse gases. The explanation for these low relative strengths is that the absorption peak of nitrogen oxide severely overlaps with water, and another peak of methane overlaps with water, carbon dioxide, and nitrogen oxide. The GWP values and the relative strengths measure GHGs in different ways: the relative strengths show warming effects during shorter time intervals and the GWP value shows warming effects during the century scale.
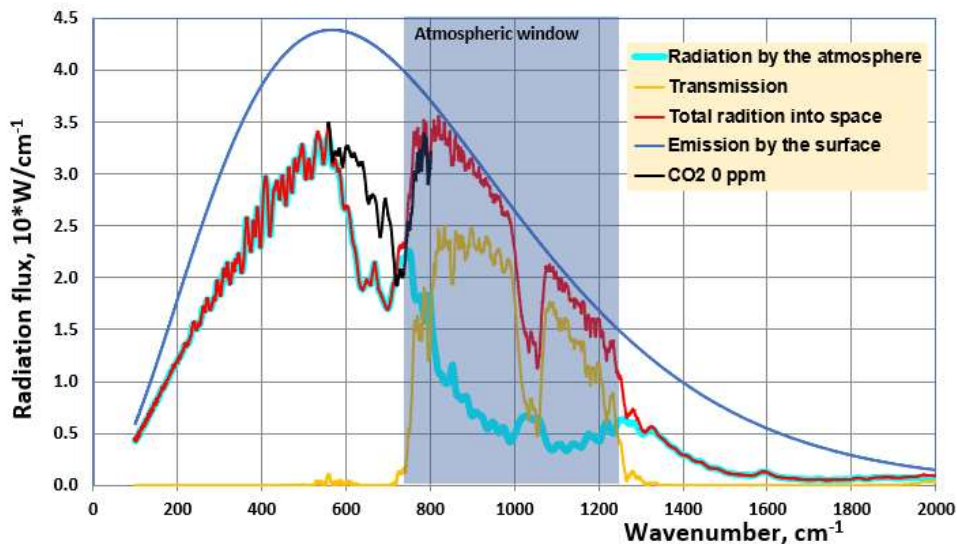

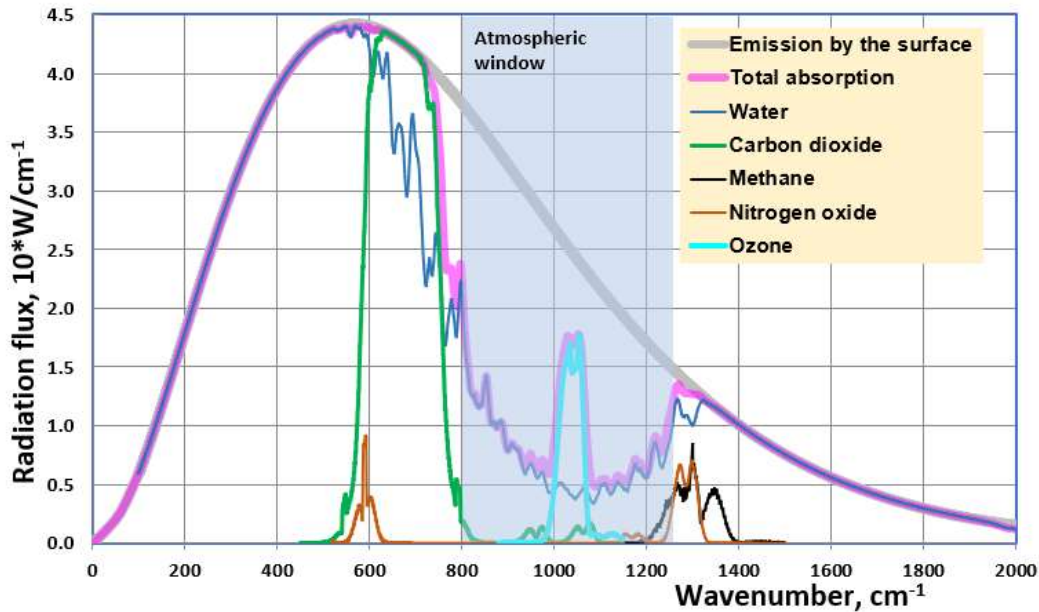**Fig. 4. OLR radiation in clear-sky conditions when carbon dioxide concentration is 393 ppm**

Fig. 5. The absorption areas of major greenhouse gases

4. CLIMATE SENSITIVITY CALCULATIONS

4.1 Effective Radiative Forcing of CO_2 Using LBL Calculations

In this study, radiative forcing calculations were carried out using five CO_2 concentrations (ppm) — 280, 393, 560, 840, and 1370 — while keeping the surface temperature at 16.3 °C under clear-sky and cloudy-sky conditions. The applied atmospheric conditions are the same as those specified in Section 3. The calculations were performed up to the altitude of 70 km, thus directly including the LW absorption effects taking place in the stratosphere.

The all-sky values have been calculated using Eq. (8). The results of different sky conditions are summarized in Table 2.

The results are also depicted in Fig. 6 showing the calculated ERF values per the

CO_2 concentration above and the corresponding warming values calculated using Eq. (5).

The final ERF results are calculated by summarizing the all-sky conditions that have been fitted into the logarithmic formula:

$$ERF = 3.83 * \ln(C/280) \qquad (11)$$

The fitting is almost perfect since the coefficient of correlation is 0.9999 and the standard error is 0.018 Wm^{-2}. The ERF value of 2xCO_2 according to Eq. (11) is 2.65 Wm^{-2}, which is practically the

same as the IRF of 2.6 Wm^{-2} of Smith et al. [13], but much smaller than the 3.93 Wm^{-2} used by the IPCC [2], and is greater than the 2.14 of [18]. The difference from the Ollila [18] value is mainly due to the cloudy-sky effects since the cloudy-sky ERF value of this study is 15.5% lower than the clear-sky value compared to 30% from the clear-sky value of [18]. The ERF values of CO_2 and the corresponding temperature values are depicted in Fig. 6.

Table 2. ERF values of CO_2 (Wm^{-2}) concentration change in different sky conditions

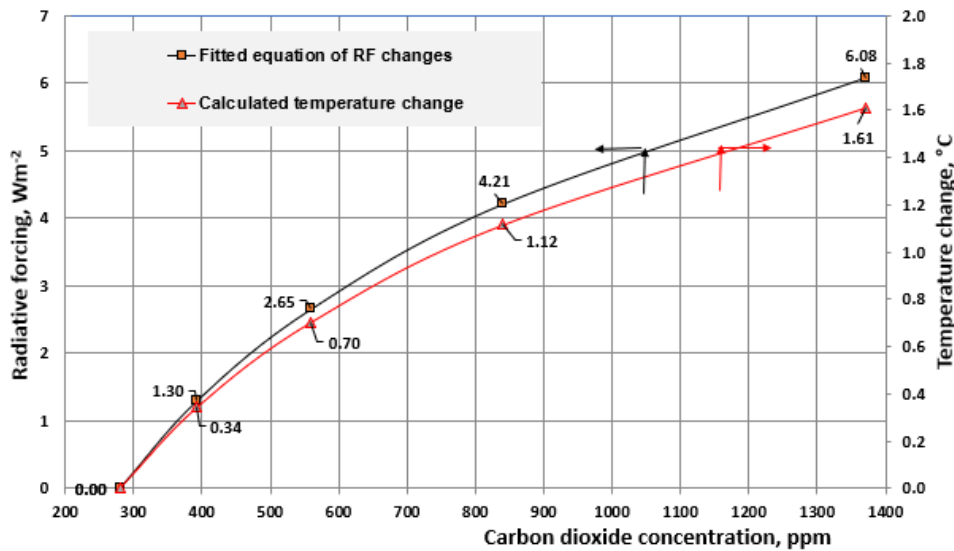| CO_2	Clear-sky				Cloudy-sky		All-sky		Strat. cooling	Total ERF
ppm	Rad.	Trans.	TOA	RF	TOA	RF	TOA	RF	RF	TOA
280	187.89	83.08	270.91	0.00	229.05	0.00	242.70	0.00	0.00	0.00
393	187.71	81.90	269.61	1.30	227.95	1.10	241.53	1.16	0.13	1.29
560	187.58	80.65	268.23	2.67	226.79	2.26	240.30	2.40	0.26	2.66
840	187.54	79.10	266.60	4.31	225.41	3.64	238.83	3.86	0.42	4.28
1370	187.73	76.93	264.66	6.24	223.77	5.28	237.10	5.59	0.60	6.20

Fig. 6. ERF changes per CO$_2$ concentration changes and the temperature changes per λ = 0.265 K/(Wm^{-2}).

4.2 Radiative Forcing of CH$_4$ and N$_2$O Using LBL Calculations

The author carried out radiative forcing calculations using 720, 1000, 1866, and 2500 ppb concentrations for CH$_4$, and 270, 324, 400, and 450 ppb concentrations for N$_2$O. The calculation methods, as well as the atmospheric and surface conditions, were the same as in the CO$_2$ calculations. The RF results are depicted in Fig. 7.

The simplified RF equation for CH$_4$ is

$$RF = -0.82715 + 0.03198 * C^{0.5} \qquad (12)$$

where C is the CH$_4$ concentration in ppb. The RF equation for N$_2$O is

$$RF = -1.3129 + 0.08474 * C^{0.5} \qquad (13)$$

where C is the N$_2$O concentration in ppb. The fitting of the RF equations has a coefficient of determination r^2 above 0.999.

The change in RF from 1750 to 2019 is 0.51 Wm^2 for CH$_4$. and 0.15 Wm^{-2}, whose values are slightly smaller than those in AR6 (IPCC, 2021): 0.54 Wm^{-2} and 0.21 Wm^{-2}.

4.3 Transient Climate Response

The transient climate response (TCR) value can be calculated using Equation (5)

$$TCR = 0.265 \ (°C/Wm^{-2}) * 2.65 \ Wm^{-2} = 0.70 \ °C \qquad (14)$$

Since the ERF and calculations are based on one specified climate condition profile, there is no statistical error, which could be used as a measure of accuracy. The IPCC [2] has reported accuracy limits of ±0.47 Wm^{-2} for their ERF values based on 10 different GCM calculations. By using this value of ERF uncertainty in this study, the uncertainty value would be 0.47 Wm^{-2} * 0.265 K/(Wm^{-2}), which is 0.13 °C. There is a smaller uncertainty in the λ value, and therefore, the final TCS can be estimated to be 0.7± 0.15 °C. This TCS value is verified and validated in Section 5.

The λ value of 0.265 (°C//Wm^{-2}) is based on the empirical radiation and temperature values of the Earth's energy balance, and it can be assessed to encompass all the feedback effects in the surface/atmosphere system for small changes in the incoming energy input regardless of whether the change is in SW$_{net}$ flux or atmospheric constituents such as CO$_2$. In this respect, the calculation basis is different from the IPCC definitions, but, as analyzed in Section 1.2, the λ calculation gives the same results for the TRC as it does for the complicated GCMs.

5. VALIDATION

Verification is a method used to compare two values calculated by different methods. Validation is the assessment of the accuracy of a

computational simulation by comparison with empirical data, and therefore, it is more valuable than verification. The validation of the ERF calculation of GHG forcing using observed values is practically impossible due to their small impacts, which other climate variables can easily mask under real climate conditions.

The radiation/temperature effects of different ERF factors can be verified both by theoretical calculations and by the CERES [25] SW radiation data. According to the GH theory, the ERF caused by $2xCO_2$ decreases the OLR flux, which causes the surface temperature (=TCS/TCR) to increase so much that the OLR returns to its original value. The ERF value of $2xCO_2$ in the clear-sky conditions is 2.679 Wm^{-2}, and by applying the λ value of 0.265 °C/(Wm^{-2}) the corresponding surface temperature increase of 0.65 °C. By using this elevated temperature, which increases the temperature profile evenly in the LBL calculation of Gats [19] under clear-sky conditions, and keeping the CO_2 concentration at 560 ppm, the $OLR_{all-sky}$ value increases from 240.302 Wm^{-2} to 242.631 Wm^{-2}. This is only 0.03% smaller than the $OLR_{all-sky}$ value of 242.702 Wm^{-2} per a CO_2 concentration of 280 ppm.

These calculations show that the required surface temperature change is the same as the temperature change in the atmosphere corresponding to the Stefan–Boltzmann energy balance calculations. The LBL calculations are

consistent, and the λ value without water feedback gives the correct OLR result.

Empirical evidence about the non-existence of constant relative humidity (RH) in real climate comes from the observed temperature and RH measurements [29]. Even though the Clausius-Clapeyron equation was a theoretical basis in the humidity calculations of early-days GCMs, nowadays the constant RH emerges as a result of the detailed hydrological cycle calculations of GCMs. Anyway, positive water feedback is still a reality in GCMs. It means that the physical connection between the total precipitable water (TPW) and RH is that RH should be constant, and the TPW should increase as temperature increases.

The global temperature according to UAH [38] increased from 1980 to 1998, but the TPW [29] decreased, and therefore, the RH decreased (Fig. 8). During the temperature pause from 2000 to 2014, when the temperature was essentially constant, the TPW increased, and the RH value decreased. These curves are identical to the curves of Fig. 8 of AR6 [2]. If the climate kept a constant RH, it should remain consistent all the time, and not only during short periods. Positive water feedback means that the water content depends on surface temperature changes without essential time delays. Fig. 8 shows that the empirical humidity observations do not support the positive water feedback theory.
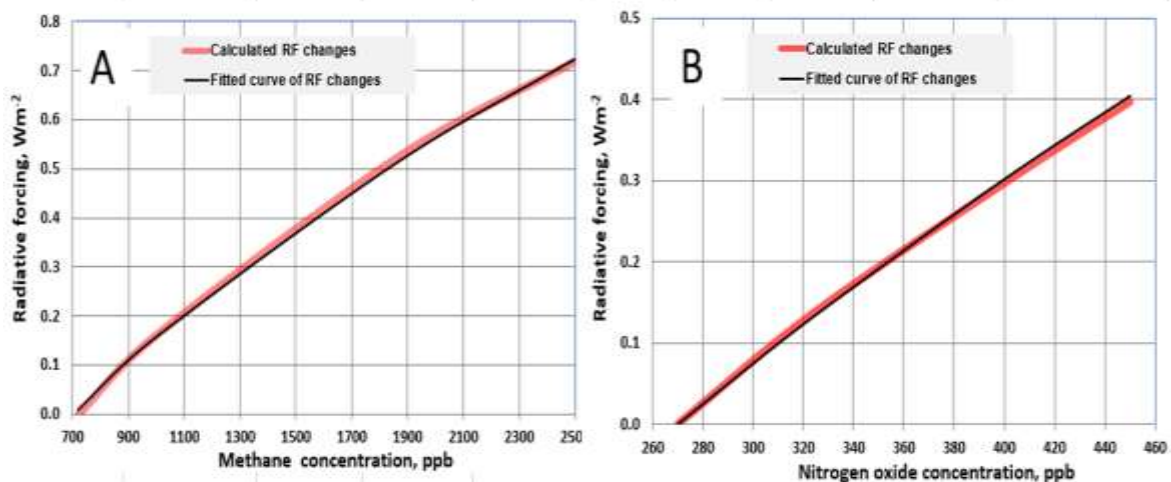

Fig. 7. A. RF changes per CH$_4$ concentration changes. A. RF changes per N$_2$O concentration changes
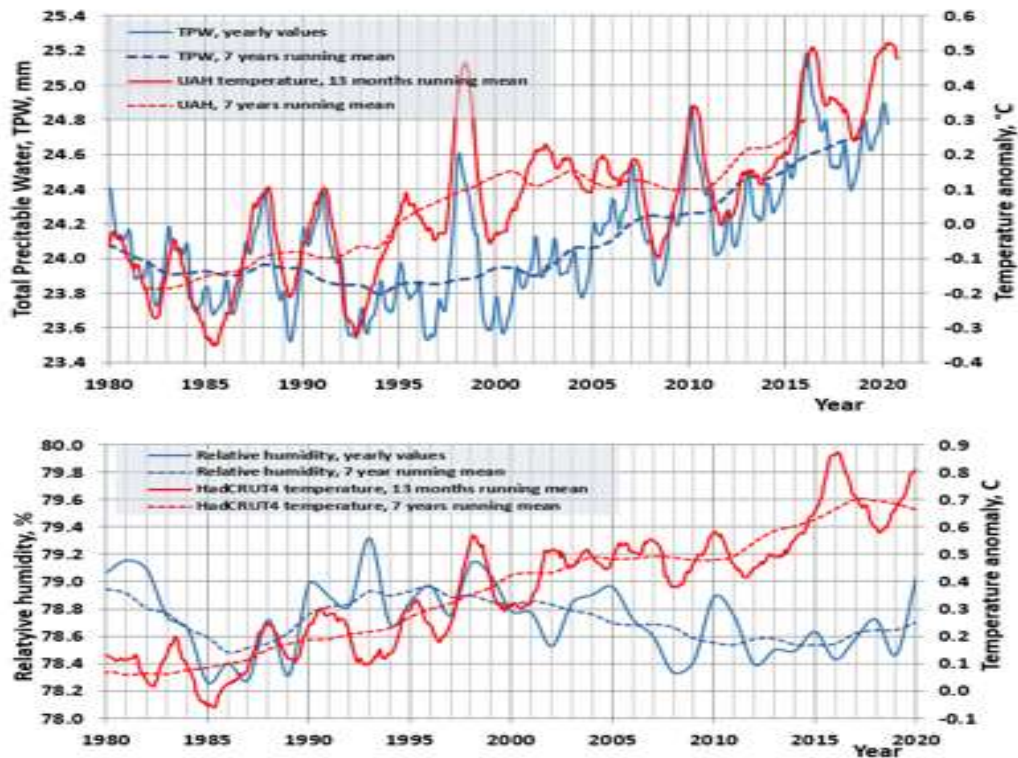
Fig. 8. A. The temperature trend and TPW (Total Precipitable Water) trends from 1980 to 2020. B. The temperature trend and Relative Humidity trends from 1980 to 2020

Only during short-term ENSO events of about two years, observed during El Nino peaks, did positive water feedback occur, and this explains why a relatively small Nino 3.4 area disturbance can have global temperature effects. About 50% of El Nino's temperature effect is due to increased atmospheric water vapor [13]. However, it is also obvious that the TPW does not stay constant, and there is an increasing trend from 2015 onward. The reasons will be commented on later.

The average values for the reference period 2008–2014 are (calculated in this study/observed in Wm^{-2}) as follows: OLR_{clear} 269.6/268.0, OLR_{cloudy} 226.5/226.5, and $OLR_{all-sky}$ 240.6/240.0. The surface temperature of 16.3 °C gives the emitted LW flux of 398 Wm^{-2}, corresponding to the Earth's energy budget value set out by Wild et al. [39], who applied the observed LW radiation values. The simulation in this study gives values very close to the observed values, both at the TOA and at the surface. The OLR flux values are remarkably close to the observations, and these small differences have no essential effects on the CO_2 concentration change calculations.

The observational spectral data in panel B of Fig. 9 of Huang and Chen [40] according to CERES [25] from August 2012 to July 2018 show average OLR spectral fluxes of 272.6 Wm^{-2} for clear-sky conditions and 241.7 Wm^{-2} for all-sky conditions. The author has simulated in this study these conditions by applying the CO_2 concentration of 401 ppm of this period and the surface temperature of 16.3 °C for the three sky conditions. The simulated $OLR_{clear-sky}$ value is 272.0 Wm^{-2} and the $OLR_{all-sky}$ is 243.6 Wm^{-2}.

The forms of spectral amplitude as a function of wavenumber are very similar between the panel A and B curves in Fig. 9. A reduction in the OLR flux values of cloudy and all-sky conditions occurs in the wavenumber zones (cm^{-1}) 300–550. 750–1000, and 1100–1300, both according to observations and in the OLR simulations. Since the CO_2 absorption zone is from 550 cm^{-1} to 750 cm^{-1}, clouds seem to have minimal effects on CO_2 absorption.

Another real validation set of calculations can be obtained by simulating the SW radiation anomaly (later SW_{net}) after 2001. The SW_{net}, according to
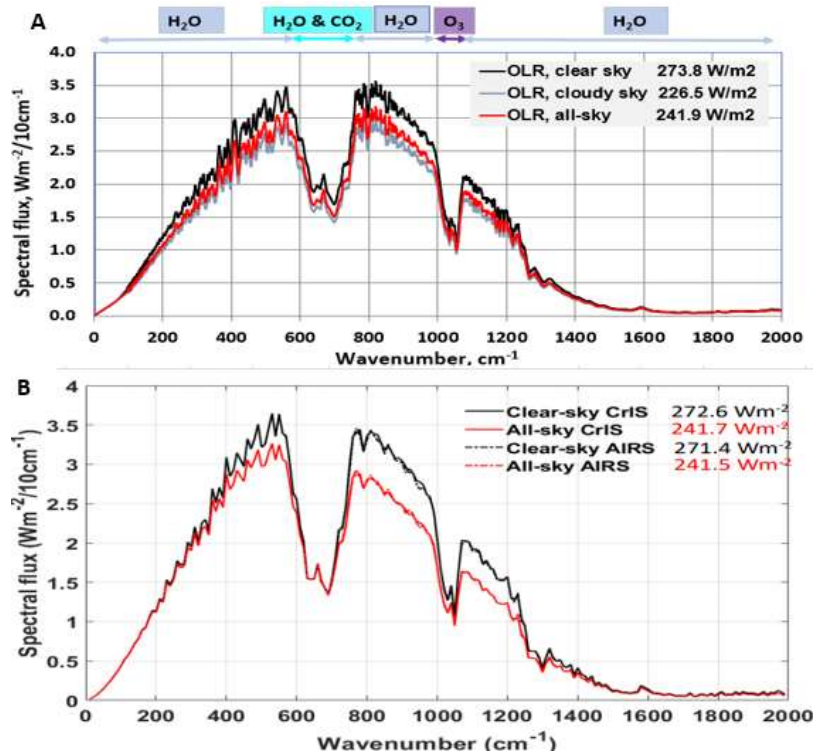
Fig. 9. OLR spectral fluxes at the TOA according to the LBL calculations of this study (panel A), and according to observed NOAA spectral fluxes (panel B) [41]. Permission to reproduce panel B of Fig. 9 has been requested from Prof. Xianglei Huang
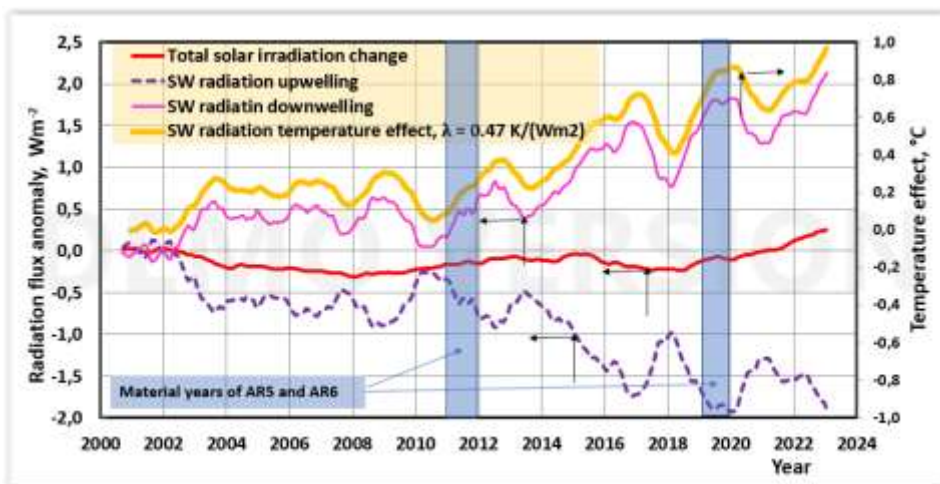

Fig. 10. Observed SW and LW radiation changes at the TOA from 2001 to 2020. The SW$_{net}$ change is the same as the SW radiation downwelling. The temperature effect of SW radiation is according to the IPCC model with water feedback

monthly values of CERES [25], is 1.75 Wm^{-2}, from 240.32 Wm^{-2} in January 2001 to 242.05 Wm^{-2} in December 2019 (Fig. 10).

This SW$_{net}$ trend with the same numerical values can be also found in Fig. 2(a) of Loeb et al. [41] and in Fig. 3 of AR6 [2]. This significant SW

anomaly of the 2000s is a reality but it has not got much attention. According to Loeb et al. [42] this SW anomaly is probably due to the changes in low-level clouds.

According to the glossary of AR5 [1], the portion of any top-of-atmosphere radiative effect that is

due to anthropogenic or other external influences, such as changes in the Sun activity, is termed instantaneous radiative forcing (IRF). An OLR increase of 1.75 Wm^{-2} would result in a surface temperature T_s increase of 0.82 °C by using the λ value of 0.47 $K/(Wm^{-2})$ of the IPCC (2021).

An LBL simulation was also carried out in this study using this increased T_s temperature of 0.88 °C (corresponding to the λ value of 0.47 $K/(Wm^{-2})$), and the CO_2 concentration of 393 ppm. The $OLR_{all-sky}$ value increased from 240.69 Wm^{-2} to 244.07 Wm^{-2}, which is 3.37 Wm^{-2} (92.6%) greater than the original SW change. It contradicts the laws of physics to suggest that the climate system would generate more energy than is coming in (240.09 + 1.75 = 241.84 Wm^{-2}), and therefore the λ value of 0.47 - 0.5 $K/(Wm^{-2})$ cannot be correct. The effects of λ values between 0.5 $K/(Wm^{-2})$ and 0.47 $K/(Wm^{-2})$ are very small.

Ollila [43] simulated the temperature effects during this period using both the IPCC's simple climate model and his simple climate model by starting temperature changes from zero in 2001, Fig. 11. The SW_{net} anomaly with the magnitude of 1.75 Wm^{-2} (the same as the calculations above) took place under real climate conditions; the observed GISS temperature change [38] was 0.46 °C. In the IPCC model, a λ value of 0.47 Wm^{-2} was applied, and the CO_2 impact was calculated using Eq. (1), but the other GHG effects were omitted due to their insignificant impact in the 20-year simulation period. For this study, the earlier simulations of the Ollila model were repeated using Eq. (5), with the λ value of 0.265 Wm^{-2}, and the ERF value of CO_2 was calculated using Eq. (11). The temperature impact dT of the ENSO effect has been calculated from the Oceanic Nino Index [44], dT = 0.1 * ONI with 6 months delay according to [45] and [43]. The dynamical time constants for the ocean were 2.74 months and for land 1.04 months according to [46] and [47].

The temperature change from 2001 to 2019 according to the IPCC model is the sum of the SW_{net} change 0.78 °C, anthropogenic drivers, 0.30 °C [2], and the ENSO effect, 0.03 °C, to give a total of 1.11 °C, meaning an error of +0.66 °C in respect to GISS data. The Ollila model is the sum of a SW_{net} change of 0.40 °C, CO_2 forcing of 0.10 °C, an ENSO effect of 0.03 °C, and cloud effects of -0.01 °C, for a total of 0.52 °C, meaning an error of +0.07°C in respect to GISS temperature. The error of the IPCC model is 840% greater than in the Ollila model. Both models follow the dynamic changes of the temperature very well confirming that the time constants of dynamics are correct.
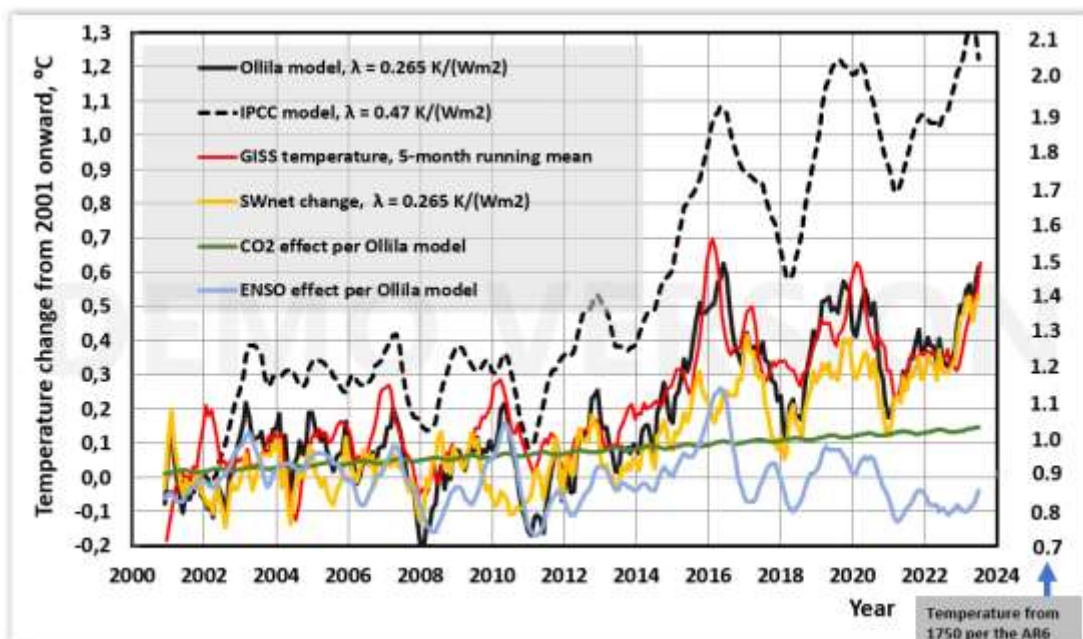

Fig. 11. Calculated temperature changes according to different models and observed temperature changes from 2001 to 2020. The SW_{net} changes are the same as in Fig. 10.

Since the SW radiation change was 1.75 Wm^{-2}, the $OLR_{all-sky}$ value change should be the same after dynamic delays. The observed $OLR_{all-sky}$ increase at the end of 2019 was 1.07 Wm^{-2}. A possible reason for the difference of 0.68 Wm^{-2} between the SW and LW radiation fluxes may be other unknown climate drivers having a temperature-reducing effect on the T_s. Some researchers are convinced that this difference is due to the slight increase in ocean heat content (OHC), which represents the bulk of the climate system's enthalpy [47] and [48]. Other reasons may be model inaccuracies and measurement problems in $OLR_{all-sky}$, which was 0.78 Wm^{-2} lower than the SW radiation flux from 2001 to 2019 according to the CERES data (2021). The dynamical simulation of the Ollila model shows that the simulated temperature changes effectively follow the observed temperature changes, indicating no increasing error from 2001 to 2020, and this result means that there was no absorption of heat into the deep ocean.

6. DISCUSSION

The $2xCO_2$ value of this study is 2.65 Wm^{-2}, which cannot be validated in real climate conditions, and it applies to all other similar studies, such as AR6 [2]. The simulation of the climate's response to the SW anomaly shows that the $2xCO_2$ impact of 2.65 Wm^{-2} fits into the overall temperature change from 2001 to 2019. Stratospheric adjustments for CO_2 forcing have been thoroughly analyzed and found to be 0.265 Wm^{-2}. The TCS/TCR value is 0.7 ±0.15 °C, based on these results.

The $2xCO_2$ value of this study is 2.65 Wm^{-2}, and this is much smaller than the ERF 3.93 Wm^{-2} of AR6 [2]. A special feature of AR6 is that the IPCC does not refer to the IRF value of 2.6 Wm^{-2} of Smith et al. [13] even though AR6 uses their rapid adjustments. It should be noted that the IRF of 2.65 Wm^{-2} given by the LBL calculations of this study is close to the 2.6 Wm^{-2} of [13]. In the second version of AR6, Table 2 shows that the IRF values of [13] varied from 2.13 to 3.09 Wm^{-2}. The IRF of this study is well within these values. It appears that the IPCC has promoted the new kernel approach paradigm but has not used its results directly.

The difference between the ERF value of 3.7 Wm^{-2} given by Smith et al. [13], and that of 2.65 Wm^{-2} of this study, is mainly due to the stratospheric cooling effect of 1.12 Wm^{-2}, which

cannot be identified in Etminan et al. [11] and in Meinshausen et al. [12]. The magnitude of the stratospheric cooling of this study is 0.265 Wm^{-2} for $2xCO_2$ and it is the result of LBL calculations. The IPCC [2] does not refer to any differences in stratospheric cooling concerning [5], [13], and [2] does not comment on the significant differences between their stratospheric cooling results in the published research papers.

It looks like the IPCC leaves the magnitude of the stratospheric cooling issue unclear. The basic principles of the IPCC are that it does not carry out its own research work, but only evaluates reviewed research studies and selects the best approach. The ERF calculation analysis of AR6 shows that the IPCC has not followed this basic principle and has carried out its own calculations. Further, its ERF value of 3.93 Wm^{-2} is about 0.2 Wm^{-2} greater than any other research paper's values, which range from 3.7 to 3.75 Wm^{-2}. In this paper, both the stratospheric cooling and warming have been calculated by applying the LBL spectral analysis method but in the AR6 [2] the magnitude is unclear, and in other research studies the method is also unclear like in Etminan et al. [11] and Meinshausen et al. [12].

There might be doubts that the LBL calculations of the Spectral Calculator are not capable enough to consider for example the chain in absorption and re-emission occurring at all levels in the atmosphere. The results of simulations of this study show that the OLR values are remarkably close to observed values by CERES satellites [25] and the total absorption by CO_2 is very close to Schmidt et al. [28]. It means that the whole chain of emissions and absorptions happening to infrared radiation from the surface to TOA in the atmosphere must be correct and they do not contain fundamental LBL calculation errors.

The study of Myhre et al. [17] used three atmospheric zones, which are the same as in the other study by Myhre et al. [5]. The TPW value of their atmosphere is 2.55 cm, which is close to the value of 2.6 cm used in this study. The calculation method of Myhre et al. [5] was the broadband model OBIR (Oslo broadband infrared), which includes cloud effects [49] and gives an OLR value of 242.3 Wm^{-2}.

The study of Etminan et al. [11] gives a $2xCO_2$ value of 3.84 Wm^{-2}. which is insignificantly greater than the result in the

original study of Myhre et al. [5]. Etminan et al. [11] used the enhanced Oslo LBL code including clouds, SW absorption, and stratospheric temperature adjustment. The Oslo LBL calculation method using the T_s temperature of 14.3 °C gives an OLR value of 234 Wm^{-2}, which is insignificantly lower than the present-day OLR values around 240 Wm^{-2}.

The calculated OLR values of this study, are remarkably close to the observed values, which is not the case with Myhre et al. [5] and Etminan et al. [11]. The question is whether this inaccuracy could explain the great differences in $2xCO_2$ values concerning this study. The LBL codes applied in these three studies are a more likely explanation. The decisive property of the LBL codes is seen in the absorption effects calculation of CO_2. This property is deeply embedded in the codes. Because the Oslo LBL code includes so many elements, parallel calculations would be needed to find any possible differences in the results.

Some studies and results indicate that the $2xCO_2$ value of 2.65 Wm^{-2} is not the only one that differs from the IPCC's value of 3.93 Wm^{-2}. For example, the 3.98 Wm^{-2} of Shi [50] was calculated under constant relative humidity conditions, which means that water feedback has duplicated the calculated ERF value. Usually, this result is referred to as if it were calculated on the same basis as other $2xCO_2$ studies. A reason for this may be that this study is not widely available, and therefore this feature has not been noticed.

The $2xCO_2$ values of three other research studies should be considered: Wijngaarden and Happer [20] found 3.0 Wm^{-2}, Miskolczi and Mlynczak [22] found 2.53 Wm^{-2}, and Harde [21] found 2.4 Wm^{-2}. Thus, after all, the $2xCO_2$ of 2.65 Wm^{-2} in this study is not the only one that deviates from the IPCC's value of 3.93 Wm^{-2}. The $2xCO_2$ values of different research studies considered by the IPCC were calculated using the Oslo LBL code, and the lower values above were calculated using different LBL codes but using the same HITRAN database.

Some researchers have reported a much lower TCS/TCR value than the 1.8 °C (likely ranging from 1.4 °C to 2.2 °C) of AR6 [2]. Miskolczi and Mlynczak [22] calculated a TCS value of 0.48 °C by simulating the CO_2 perturbations in three climate zones and summarizing them globally.

Harde [21] utilized the ERF value of 2.4 Wm^{-2} of $2xCO_2$, and his CS value was 0.6 °C with feedback, which he compared to the ECS value of the IPCC. The TCR values of Wijngaarden and Happer [20] were 2.3 °C, derived by applying constant relative humidity, and 1.4 C, derived with fixed absolute humidity, which is higher than those of the IPCC [2]: 1.8 °C and 1.2 °C. These results mean that there are still significant gaps between the climate sensitivity values of different studies, which cannot be explained by the identified flaws in calculation methods.

When applying ERF, the values of warming given by AR5 [1] and AR6 [2] increased according to the simple model $dT = \lambda * ERF = 0.47$ K/(Wm^{-2}) * $(2.70 - 2.34)$ $Wm^{-2} = 0.17$ °C. The climate driver of "Aerosols and clouds" decreased from -0.82 Wm^{-2} in 2011 to -1.0 Wm^{-2}, meaning that the IPCC has not considered any positive SW radiation increase during the 2000s. A critical reading of AR6 reveals that the SW radiation anomaly from 2001 to 2020 has been notified in Fig. 3 [2] exactly in the same way as depicted in Fig. 9 and 10. Fig. 3 also reveals that GCMs cannot estimate this kind of SW radiation anomaly. The IPCC [2] decided to omit this anomaly in its warming calculations from 1750 to 2019. This exclusion of the SW radiation warming effect creates an error of 0.47 * 1.61 = 0.76 °C. There would have been another way to solve this problem by applying direct observational SW values in the same way as the IPCC applies direct CO_2 concentration observations in the warming calculations.

The model-calculated warming value from 1750 to 2019 is 1.29 °C [2]. Adding the warming of 0.76 °C due to the SW radiation anomaly would increase the model-calculated temperature to 2.05 °C. One can only speculate, why this effect has not been included.

7. CONCLUSIONS

The most convincing result of this study is the value 0.265 K/(Wm^{-2}) of the climate sensitivity parameter λ. meaning that there is no water feedback in the climate except for short-term climate disturbances such as ENSO events. The λ value of 0.47 K/(Wm^{-2}) applied by the IPCC [2] does not hold up to theoretical analysis, LBL calculations, or tests using the real climate disturbance of the SW anomaly from 2001 to 2019.

The validation of the climate sensitivity parameter λ value of 0.265 K/(Wm^{-2}) has a sound scientific basis. The value of 0.47 K/(Wm^{-2}), meaning positive water feedback, gives erroneous results in tests run with LBL verification calculations and in real climate simulations. The λ value of this study, 0.265 K/(Wm^{-2}), passes verification/validation tests with insignificant errors. A striking feature of the λ value of 0.47 - 0.50 K/(Wm^{-2}) is that it does not pass a naturally occurring empirical test, as shown by the SW radiation anomaly from 2001 to 2020.

The other essential result of this study are ERF calculation of CO_2 according to eq. (10) that ERF = 3.83 * ln(C/280), RF calculation CH_4 according to eq. (12) that RF = -0.82715 + 0.03198 * C$^{0.5}$, the RF calculation of N_2O according to eq. (13) that RF = -1.3129 + 0.08474 * C$^{0.5}$, and the TRC value of 0.70 °C. The forms of ERF and RF formulas are similar to those reported by the IPCC but the numerical values are different.

COMPETING INTERESTS

Author has declared that no competing interests exist.

REFERENCES

1. IPCC AR5, Anthropogenic and natural radiative forcing, in Climate Change 2013: The Physical Science Basis. Contribution of Working Group I to the Fifth Assessment Report of the Intergovernmental Panel on Climate Change, edited by T. F. Stocker et al., Cambridge Univ. Press, Cambridge, U. K., and New York; 2013.
2. IPCC AR6, Climate Change 2021, The Physical Science Basis. Contribution of Working Group I to the Sixth Assessment Report of the Intergovernmental Panel on Climate Change, Cambridge Univ. Press; 2021.
3. IPCC TAR, Climate Change 2001, The Physical Science Basis. Contribution of Working Group I to the Third Assessment Report of the Intergovernmental Panel on Climate Change, Cambridge Univ. Press, Cambridge, U.K., and New York; 2001.
4. IPCC AR4, Climate Change 2007, The Physical Science Basis. Contribution of Working Group I to the Fourth Assessment Report of the Intergovernmental Panel on Climate Change, Cambridge Univ. Press, Cambridge, U.K., and New York; 2007.
5. Myhre G, Highwood EJ, Shine KP, Stordal F. New estimates of radiative forcing due to well mixed greenhouse gases. Geophys Res Lett 1998;25:2715-2718.
6. Manabe S and Wetherald RT. Thermal equilibrium of the atmosphere with the given distribution of relative humidity. J Atm Sci. 1967;24(3):241-259.
7. Ramaswamy V, Collins W, Haywood J, Lean J, Mahowald N, Myhre G, et al. Radiative Forcing of Climate: The historical evolution of the radiative forcing concept, the forcing agents and their quantification, and applications. Meteorol Monogr. 2019;59(1):14.1-14.101.
8. Goessling HF and Bathiany S. Why CO_2 cools the middle atmosphere – a consolidating model perspective. Earth Syst Dyn. 2016;7(3):697–715.
9. Ohmura A. Physical Basis for the Temperature-Based Melt-Index Method. J Appl Meteorol Climatol 2001;40:754-761.
10. Ollila A. Warming effect reanalysis of greenhouse gases and clouds. Phys Sc Int. J 2017;13(2):1-13.
11. Etminan E, Myhre G, Highwood EJ, Shine KP. Radiative forcing of carbon dioxide, methane, and nitrous oxide: A significant revision of methane radiative forcing. Geophys Res Lett 2016;43:12614-12636.
12. Meinshausen M, Nicholls MRJ, Lewis J, Gidden MJ, Vogel E et al. The shared socio-economic pathway (SSP) greenhouse gas concentrations and their extensions to 2500. Geosci Model Dev. 2020;13:3571–3605.
13. Smith CJ, Kramer RJ, Myhre G et al. Understanding rapid adjustments to diverse forcing agents. Geophys Res Lett 2018;45:2023–12031.
14. Huang Y and Ramaswamy V. Effect of the temperature dependence of gas absorption in climate feedback. J Geophys Res 2007; 112(D7).
15. Chung ES, Soden BJ. An assessment of direct radiative forcing, radiative adjustments, and radiative feedbacks in coupled ocean–atmosphere models. J Clim 2015;28(10):4152–4170.
16. HITRAN. High-Resolution Transmission Molecular Absorption database, Harvard-Smithsonian Center for Astrophysics; 2021. Available:https://www.cfa.harvard.edu/hitran/
17. Myhre G, Stordal F, Gausemel I, Nielsen CJ, Mahieu E. Line-by-line calculation of thermal infrared radiation for global

condition: CFC-12 as an example. J Quant Spectros Radiat Transf. 2016; 97:317–331.

18. Ollila A. The potency of carbon dioxide (CO_2) as a greenhouse gas. Dev in Earth Sc 2014;2:20-30.

19. Gats. Spectral calculations tool, Gats Inc; 2021.
Available:http://www.spectralcalc.com/info/help.php.

20. Wijngaarden W and Happer W. Dependence of Earth's thermal radiation on five most abundant greenhouse gases. Arxiv.org/pdf/2006.03998.pdf.

21. Harde H. Radiation and heat transfer in the atmosphere: A comprehensive approach on a molecular basis. Int J Atmos Sci. 2013;ID 503727.

22. Miskolczi FM and Mlynczak MG. The greenhouse effect and the spectral decomposition of the clear-sky terrestrial radiation. Idöjaras 2004;108: 209-251.

23. Ramanathan V, Cicerone R, Singh H, Kiehl I. Trace gas trends and their potential role in climate change. J Geophys Res 1985; 90:5547-5566.

24. MODTRAN. Moderate resolution atmospheric transmission computer code, Spectral Science Inc; 2020.
Available:http://modtran.spectral.com/

25. CERES. CERES EBAF-TOA Data, The National Oceanic and Atmospheric Administration (NOAA); 2021.
Available:https://ceres-tool.larc.nasa.gov/ord-tool/jsp/EBAFTOA41Selection.jsp

26. Mlawer EJ, Payne VH, Moncet J-L, Delamere JS, Alvarado MJ, Tobin DC. Development and recent evaluation of MT_CKD model of continuum absorption. Philos Trans, Math Phys Eng Sci. 2012; 370:2520-2556.

27. Kiehl JT, Trenberth KE. Earth's annual global mean energy budget. Bull Amer Meteor Soc 1997;90:311-323.

28. Schmidt GA, Ruedy RA, Miller RL. Attribution of the present-day total greenhouse effect. J Geophys Res. 2010; 115:D20106.

29. NOAA. NCEP/NCAR Reanalysis Data; 2021.
Available:https://www.esrl.noaa.gov/psd/cgi-bin/data/timeseries/timeseries1.pl

30. NOAA. Greenhouse gas concentration data; 2021.
Available:https://gml.noaa.gov/ccgg/trends/data.html

31. Huang B, Angel W, Boyer T, Cheng L, Chepuring G et al. Evaluation SST analyses with independent ocean profile observation. J Clim. 2018;36:5015-5030.

32. Bellouin N, Boucher O, Haywood J, Shekar Reddy M. Global estimate of aerosol direct radiative forcing from satellite measurement. Nature. 2003;438:1138-1141.

33. Zhang T, Rossow WB, Lacis AA, Oinas V. Calculations of radiative fluxes from the top of atmosphere based on ISCCP and other global data sets: Refinements of the radiative model and the input data. J Geo Res 2004;109:1149-1165.

34. Wang J, Rossow WB, Zhang Y. Cloud vertical structure and its variations from a 20-yr global rawinsonde dataset. J Climate. 2000;13:3041-3056.

35. Ollila A. The greenhouse effect calculations by an iteration method and the issue of stratospheric cooling. Phys Sc Int J. 2020;24(2):1-20.

36. Bekki S and Savarino J. Ozone and stratospheric chemistry. Ed. White WM, Encyclopedia of geochemistry. Springer International Publishing. 2016;12,978-3-319-39193-9;.

37. Philipona R, Mears C, Fujiwara M, Jeannet P, Thorne P, Bodeker G, Haimberger L, Hervo M, Popp C, Romanens G, Steinbrecht W, Stübi R, Van Malderen R. Radiosondes show that after decades of cooling, the lower Stratosphere is now warming. J Geophys Res Atmos 2018; 123:12509-12522.

38. GISS. Land-ocean temperature index of NASA; 2021.
Available:https://data.giss.nasa.gov/gistemp/tabledata_v4/GLB.Ts+dSST.txt

39. Wild M, Hakuba MZ, Folini D, Dörig-Ott P, Schär C, Kato S, Long CN. The cloud-free global energy balance and inferred cloud radiative effects: an assessment based on direct observations and climate models. Clim Dyn. 2019;52:4787–4812.

40. Huang X and Chen X. A synergistic use of hyperspectral sounding and broadband radiometer observations from S-NPP and Aqua., Fall 2020 NASA Sounder Science Team Meeting October 05.

41. Loeb NG, Johnson GC, Thorsen TJ, Lyman JM, Rose FG, Kato S. Satellite and ocean data reveal marked increase in Earth's heating rate. Geophys Res Lett .2021;48,e2021GL093047.

42. Loeb NG, Thorsen TJ, Norris JR, Wang H, Su . Changes in Earth's energy budget during and after the "pause" in global warming: An observational perspective. Climate. 2018;6:62.

43. Ollila A. The pause end and major temperature impacts during super El Niños are due to shortwave radiation anomalies. Phys Sc Int J. 2020;24(2):1-20.

44. ONI. Oceanic Nino Index (ONI), NOAA; 2021.
Available:https://ggweather.com/enso/oni.htm.

45. Trenberth KE and Fasullo JT. An apparent hiatus in global warming? Earth's Future. 2013;1:19-32.

46. Stine AR, Huybers P, Fung IY. Changes in the phase of annual cycle of surface temperature. Nature. 2009;457: 435-441.

47. Kauppinen J, Heinonen JT, Malmi PJ. Major portions in climate change: Physical approach. Ph Sc Int Jl. 2011;9(4):1-14.

48. Dübal H-R, Vahrenholt F. Radiative Energy Flux Variation from 2001–2020. Atmosphere 2021;12:1297.

49. Myhre G, Stordal F. Role of spatial and temporal variations in the computation of radiative forcing and GWP. J Geophys Res. 1997;102:11181-11200.

50. Shi G-Y. Radiative forcing and greenhouse effect due to the atmospheric trace gases. Sc in China Ser B. 1992;35:217-229.

Peer-review history:
The peer review history for this paper can be accessed here:
https://www.sdiarticle5.com/review-history/109808